

Dislocation displacement field at the surface of InAs thin films grown on GaAs(110)

J. G. Belk

*Semiconductor Materials IRC, Imperial College, London SW7 2BZ, United Kingdom
and Department of Chemistry, Imperial College, London SW7 2AY, United Kingdom*

D. W. Pashley

Department of Materials, Imperial College, London SW7 2AZ, United Kingdom

B. A. Joyce

Semiconductor Materials IRC, Imperial College, London SW7 2BZ, United Kingdom

T. S. Jones*

*Semiconductor Materials IRC, Imperial College, London SW7 2BZ, United Kingdom
and Department of Chemistry, Imperial College, London SW7 2AY, United Kingdom*

(Received 6 July 1998)

Scanning tunneling microscopy topographic images have been used to obtain the dimensions of the strain field detected at the surface of InAs thin films grown on GaAs(110) substrates by molecular-beam epitaxy. The displacement of atoms in the film due to the edge dislocation strain field has been obtained by measuring the depth and lateral dimensions of the surface response as a function of InAs thickness (≤ 30 ML). Several models based on elasticity theory are used in an attempt to reproduce the experimental measurements. Only models containing a free epitaxial layer surface produce good quantitative agreement and the experimentally observed decrease in vertical displacement is found to be largely a consequence of strain field superposition due to the increasing width of the strain field originating from adjacent dislocations. [S0163-1829(98)06548-5]

I. INTRODUCTION

A misfit dislocation constitutes a substantial discontinuity of the crystal lattice that accommodates the misfit stress between a thin film and the substrate. The deformation is not confined to the core and leads to deformation of a relatively large volume of the film and substrate lattices around the dislocation. The magnitude of the displacement field can be reproduced using elasticity theories and constitutes small ($< \sim 1$ Å) shifts in the position of each atom under the influence of the dislocation strain field. The displacement field accounts for one of the major contrast mechanisms in transmission electron microscopy (TEM) micrographs containing dislocations and it can be inspected directly, to some degree, by cross-sectional high-resolution electron microscopy (HREM).¹ Scanning tunneling microscopy (STM) also provides direct images of the displacement field, this time at the surface of the film, although the data can generally be interpreted in a straightforward fashion since the microscope simply profiles the surface topology.²⁻⁶ The strong dependence of the tunneling current on tip-sample separation means the vertical resolution of STM (~ 0.1 Å) is ideal for resolving the subtle elastic displacements involved.

The first STM study of dislocations was made by Stalder *et al.*^{3,7} for metallic CoSi₂ layers grown on Si(111) and Si(001). The tensile strain in this system led to the observation of protruding lines at the surface due to an “extra” column of atoms in the film. For a film thickness range of ~ 180 Å, the experimentally observed vertical displacement remained constant at ~ 0.6 Å for Si(111) and varied between 1.1 and 2.2 Å for Si(001), while the lateral extent of this

vertical displacement increased and was, coincidentally, roughly equal in magnitude to the film thickness. Classical elasticity theory reproduced the full width at half-maximum (FWHM), but underestimated the vertical displacement at 0.35 Å for Si(111) and 0.6 Å for Si(001), although this too was independent of film thickness; the CoSi₂ layer was assumed to be highly deformable and the maximum possible Poisson ratio of 0.5 was used. In addition to the limitations of classical elasticity theory, which applies to infinite media without a free surface, electronic contributions to the measured profiles were suggested to contribute to the poor agreement with experiment. Further attempts were made to reproduce theoretically the measured surface response by employing a molecular dynamics simulation of a dislocation containing slab of a PtNi alloy.^{8,9} Although partially successful in terms of an order of magnitude agreement, the sensitivity of the simulation to its input parameters (temperature and interatomic potentials) and the complexity of the dislocation network was problematic.

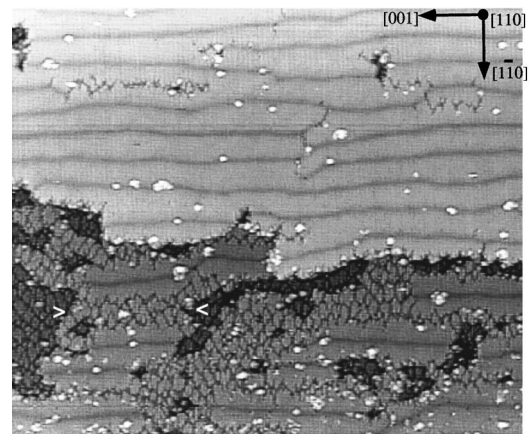
The earliest STM observation of buried dislocations in semiconducting materials was for 10 ML Ge films grown on Si(111), using an antimony surfactant to maintain a two dimensional (2D) surface morphology.^{2,10} Surface depressions with a depth of ~ 0.3 Å were observed, but these were not seen at thicker (28 ML) Ge film thickness. More recently, Springholz and co-workers¹¹⁻¹³ have analyzed the displacement field at the surface of EuTe films grown on PbTe(111). Classical elasticity theory was modified to include the presence of an unconstrained free surface by the method of image forces and expressions were derived for the displacement field at the surface. The main results for edge dislocations

were that the vertical displacement was independent of film thickness, at a value of (b/π) where $b=|\mathbf{b}|$, the Burgers vector, while the FWHM increased, broadly consistent with the findings of Stalder *et al.*^{3,7} For other systems, such as Ge/Si(111) Ref. 2 and Fe/W(110),¹⁴ the measured vertical displacement was found to decrease with increasing film thickness.

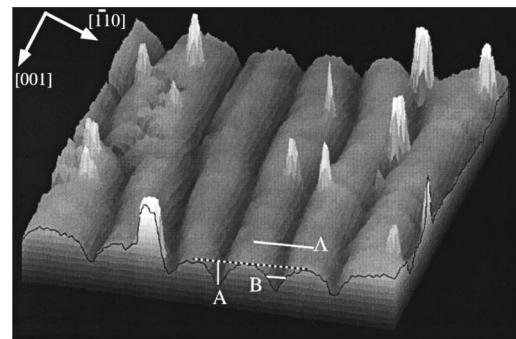
In this paper, we use STM images of InAs films grown on GaAs(110) by molecular-beam epitaxy (MBE) to analyse the atomic displacements due to the strain field around the ideal edge dislocations ($\mathbf{b}=a_0/2[1\bar{1}0]$, $\mathbf{u}=[001]$) formed near the interface. The InAs/GaAs(110) system is an ideal choice for investigation by STM since it grows in a layer-by-layer 2D mode for all film thicknesses,^{15,16} in contrast to the Stranski-Krastanov 3D behavior exhibited by InAs/GaAs(001).¹⁷ We have recently shown that the InAs/GaAs(110) growth mechanism involves the coalescence of a close packed array of 2D surface islands associated with the formation of pure edge misfit dislocations,^{16,18} an observation we have also made for InAs films grown on GaAs(111)A.⁵ For InAs/GaAs(110), a linear array of edge dislocations with Burgers vectors $\mathbf{b}=a_0/2[1\bar{1}0]$ and line directions $\mathbf{u}=[001]$ is formed, while a hexagonal network is established at the InAs/GaAs(111)A interface, which also contains partial dislocations.⁶ The simpler (110) system is clearly the most suitable for an initial investigation of the dislocation displacement fields. Several models based on classical elasticity theory are used to analyze the experimental data and the most appropriate is one recently proposed by Bonnet^{19,20} for application to any system of interfaces *which may include surfaces*. The theory is based on the properties of the differential equations of classical elasticity for periodic solutions using a Fourier series analysis and it is the first time it has been used in a detailed analysis of high-resolution STM images of a thin film.

II. EXPERIMENTAL

The samples were prepared and analysed in a combined MBE-STM facility (DCA, Finland/Omicron GmbH, Germany) equipped with reflection high-energy electron diffraction (RHEED) for *in situ* monitoring of growth. Epiready, singular n^+ Si-doped GaAs(110) substrates (American Xtal Technology) were used and each one was mounted on a molybdenum block and introduced into the vacuum chamber without any further *ex situ* preparation, prior to thermal cleaning at $\sim 300^\circ\text{C}$. Following removal of the surface oxide layer at $600\text{--}640^\circ\text{C}$ under an As_2 flux, a 10-ML-thick homoepitaxial buffer layer of GaAs was grown at a substrate temperature of 520°C and an As/Ga atomic flux ratio of 10:1.²¹ The Ga and As_2 fluxes were calibrated using RHEED intensity oscillations during the homoepitaxial growth of GaAs(001). Before InAs deposition, smooth surfaces of GaAs were obtained by annealing at 580°C to minimize the substrate step density.²² The deposition of InAs was performed at a substrate temperature of $420\text{--}480^\circ\text{C}$ and at a rate of 0.125 ML s^{-1} . These deposition conditions were chosen to ensure both a negligible InAs desorption rate (significant above $\sim 530^\circ\text{C}$) and a sufficiently high surface mobility for the deposited In. The nominal InAs layer thicknesses studied ranged from 1 to 30 ML and transmission-type dif-



(a)



(b)

FIG. 1. (a) A plan view, filled states STM image ($1000 \times 850 \text{ \AA}$) of a 5-ML InAs film grown on GaAs(110) at 420°C . The buried edge dislocations manifest themselves as the dark depressions along $[001]$. (b) A perspective view, filled states STM image ($380 \times 380 \text{ \AA}$, greyscale range $0\text{--}2 \text{ \AA}$) of the InAs/GaAs(110) surface indicating the principal quantities measured from the STM data for the edge dislocation array: A = vertical displacement, B = lateral width at half-maximum, and Λ = dislocation separation.

fraction spots never appeared in the RHEED pattern, consistent with 2D layer-by-layer growth throughout. Following deposition of InAs, the samples were transferred rapidly into the STM chamber, and once the sample had been cooled to room temperature, STM images were obtained using tunneling currents of $0.05\text{--}0.2\text{ nA}$ and a sample bias of $|V_b| = 2\text{--}4\text{ V}$.

III. RESULTS

A filled states STM image of a 5-ML InAs film deposited on GaAs(110) at 420°C is shown in Fig. 1(a). The dark horizontal bands running along $[001]$ are depressions at the surface due to the buried edge dislocations, which relieve strain along $[1\bar{1}0]$. The nucleation of the dislocations and morphological details have been discussed in detail elsewhere.^{16,18} Images of this type were analyzed at different film thicknesses (up to 30 ML) to provide a measure of the vertical surface displacement (A), the lateral FWHM (B), and the dislocation spacing (Λ): the three measurements are defined more clearly in the perspective view STM image shown in Fig. 1(b). All raw measurements were subject to slight adjustments of the order of $5\text{--}20\%$ to reflect the fine

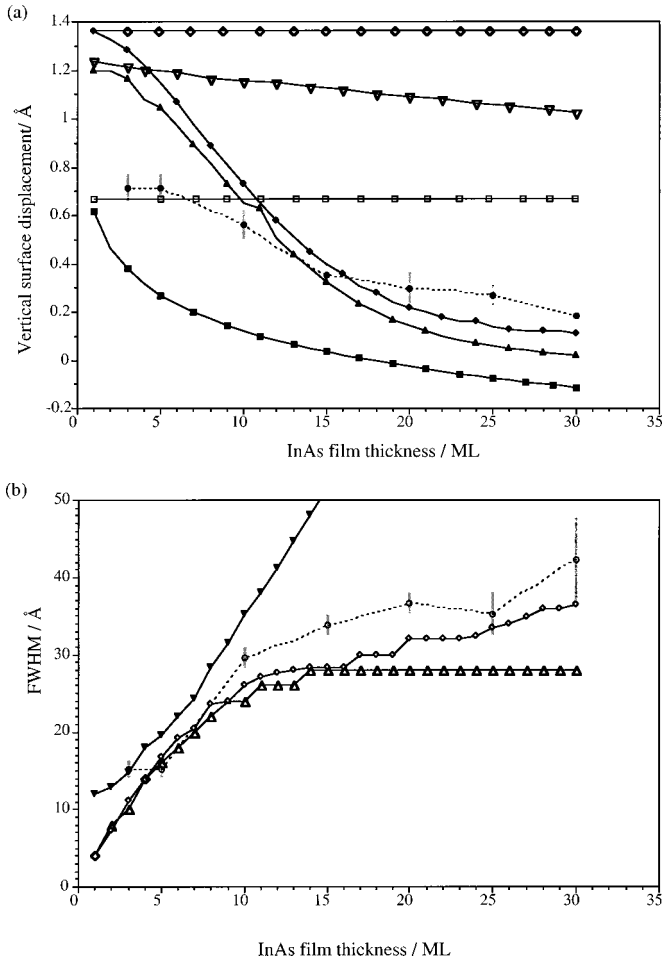


FIG. 2. (a) The experimental negative vertical displacement (\cdot) obtained from STM images of InAs/GaAs(110) as a function of InAs thickness. Also shown are the results obtained from the various theoretical methods discussed in Sec. IV; classical elasticity theory (\square , Poisson ratio=0.5; \blacksquare , Poisson ratio=0.27); Springholz model (\blacklozenge , dislocation array; \diamond , single dislocation); Bonnet model (\blacktriangle , dislocation spacing=60 Å, ∇ , dislocation spacing=1000 Å). (b) The experimental FWHM (\circ) obtained from STM images of InAs/GaAs(110) as a function of InAs thickness. Also shown are the results obtained from the various theoretical methods discussed in Sec. IV; Springholz model (\diamond , dislocation array), Bonnet model (\triangle dislocation spacing=60 Å; \blacktriangledown , dislocation spacing=1000 Å).

calibration of the (x,y,z) piezodrives, which can be established by measuring the dimensions of surface objects with a known size, e.g., step heights (z), or atom/reconstruction (x,y) periodicities.

Plots of the vertical surface displacement and FWHM are shown in Fig. 2 as a function of InAs film thickness. The initial depth of the dark lines, following their nucleation, is about 0.7 Å and this decreases to coincide with the STM vertical resolution limit of 0.1 Å by approximately 30 ML [Fig. 2(a)]. The FWHM increases from 15 to around 30–40 Å, a figure that appears to be an upper limit [Fig. 2(b)]. Both quantities are initially independent of film thickness in the 3–5 ML range during which the dislocation network is becoming established. Given the errors in the measurements, largely due to irregularities in the dislocation network, the spacing of the dislocations, Λ , remains essentially constant throughout the whole range of film thicknesses studied (Fig.

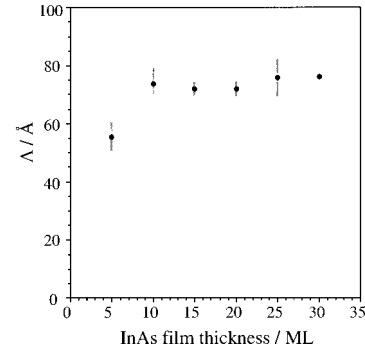


FIG. 3. The dislocation spacing (Λ) measured by STM along $[1\bar{1}0]$ as a function of InAs film thickness for InAs/GaAs(110).

3) and is close to the value of 59.5 Å predicted from the +7.2% lattice misfit. There is, therefore, little residual strain along the $[1\bar{1}0]$ direction [also indicated by RHEED Ref. 18] since the lattice relaxation promptly attains 100% once the dislocation network is completed at approximately 5 ML thickness.

IV. THEORETICAL ANALYSIS

Three theoretical treatments were used to analyze the experimental data. The common procedure was to calculate the lateral and vertical atomic displacements in the substrate and the film within a Cartesian frame (x_1, x_2) , corresponding physically to a $[001]$ cross section, namely $u_1(x_1, x_2)$ and $u_2(x_1, x_2)$. Three sets of data were then obtained; (i) the nominal atomic positions before displacement (x_1, x_2) , (ii) the atomic displacements themselves, $u_1(x_1, x_2)$ and $u_2(x_1, x_2)$, and (iii) the updated atom coordinates after displacement $[x_1 + u_1(x_1, x_2), x_2 + u_2(x_1, x_2)]$.

A. Classical elasticity theory

Expressions for the vertical (x_2 direction parallel to $[110]$) and lateral (x_1 direction parallel to $[1\bar{1}0]$) displacements obtained through classical elasticity theory are generally taken from the texts of either Nabarro²³ or Hirth and Lothe.²⁴ The theory describes a single edge dislocation of magnitude $b = |\mathbf{b}|$, located at the origin $(x_1=0, x_2=0)$ at the interface between two infinite materials with a Poisson ratio ν [Fig. 4(a)]. For each film or substrate atom, with coordinates (x_1, x_2) , the small displacements in the lateral (u_1) and vertical (u_2) sense are given by

$$u_1 = \frac{-(1-2\nu)b}{8\pi(1-\nu)} \ln\left(\frac{x_1^2 + x_2^2}{b^2}\right) + \frac{bx_x^2}{4\pi(1-\nu)(x_1^2 + x_2^2)}, \quad (1)$$

$$u_2 = \frac{bx_1x_2}{4\pi(1-\nu)(x_1^2 + x_2^2)} - \frac{b}{2\pi} \arctan\left(\frac{x_1}{x_2}\right). \quad (2)$$

The displacement field for each atom $\{x_1 + u_1(x_1, x_2), x_2 + u_2(x_1, x_2)\}$ around a single edge dislocation is shown in Fig. 5 for an InAs Poisson ratio, $\nu_{\text{InAs}}=0.27$. The theory is successful in reproducing the general aspects of the problem, i.e., two additional (220) columns in the substrate constitute the core of the edge dislocation, inducing a depression of

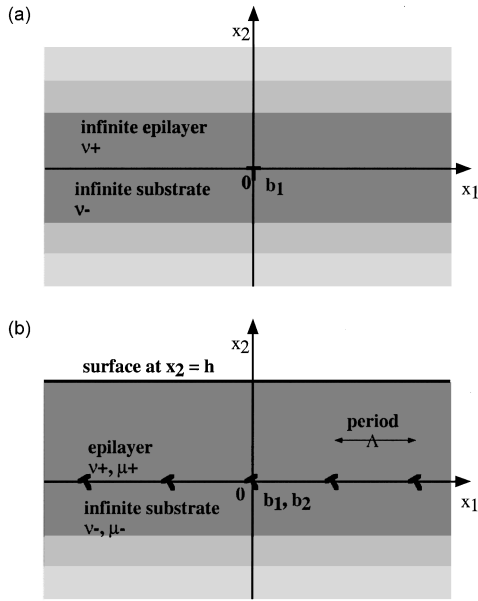


FIG. 4. (a) Schematic diagram describing the single dislocation system used in the classical elasticity theory (Sec. IV A). The dislocation line itself runs perpendicular to the plane of the figure in the x_3 direction (parallel to [001]). The film and substrate are both infinite and each is described by their respective Poisson ratio. The edge dislocation Burgers vector has a magnitude b_1 in the x_1 direction. (b) Schematic diagram describing the dislocation system used in the Bonnet model (Sec. IV C). The extra parameters compared to (a) are an epilayer surface, at $x_2 = h$, the dislocation spacing along x_1 , Λ , a Burgers vector described in three dimensions, $\mathbf{b} = (b_1, b_2, b_3)$, and the shear moduli for the epilayer ($\mu+$) and substrate ($\mu-$).

atoms above the core in the (infinite) film (u_2 negative), plus lateral shifts due to regions of local tension and shear in the film, and a region of local compression in the substrate.

The theory breaks down, however, once quantitative comparison is made between u_2 (in successive layers in the film above the dislocation; $x_1 = 0, 1 < x_2 < 30$ ML) and the corresponding surface vertical displacements measured by STM

[Fig. 2(a)]. One of the major difficulties inherent in this theory is that u_1 is logarithmically divergent for large values of x_2 [Eq. (1)]. Furthermore, for InAs film thicknesses > 16 ML, the displacement changes sign (u_2 becomes positive), which has no physical basis for an edge dislocation relieving compressive strain.

A second plot using classical elasticity theory is also shown in Fig. 2(a) for which a value of $\nu_{\text{InAs}} = 0.5$ was chosen to correspond to a system where there is no resistance to vertical displacement. The vertical displacement remains constant with film thickness at $u_2 \approx -0.68 \text{ \AA}$ and the displacement field does not diverge because the first term in u_1 vanishes [Eq. (1)]. This result is consistent with the findings of some other groups for metallic systems,^{3,13} but a clear trend of the experimental InAs/GaAs(110) vertical displacement is its decrease with film thickness, falling below the STM vertical resolution limit of $\sim 0.1 \text{ \AA}$ at ~ 35 ML. Although the strain field is long range, it is not infinite in its sphere of influence²⁵ and the dislocation stress fields are inversely proportional to distance.²⁶ It is important to consider what proportion of the decline in vertical displacement is due directly to the increase in FWHM and this is addressed in detail in Sec. IV C.

B. Modifications to classical elasticity theory

From the two classical elasticity theory plots in Fig. 2(a), it is clear that the experimental data can be accounted for by an intermediate choice for the InAs layer Poisson ratio of between 0.5 and 0.27; the remaining two parameters in the theory, the magnitude of the Burgers vector and the atom coordinates, are both fixed. An edge misfit dislocation exerts a longitudinal force parallel to the interface to compensate for the lattice mismatch and the elastic displacement of atoms in the vertical direction is, therefore, a consequence of the orthogonal *transverse* strain. Increasing the Poisson ratio above the bulk value mimics the presence of a free surface in the classical elasticity theory by making the epitaxial layer more deformable in the vertical direction. Table I gives the values of the Poisson ratio (ν_{fit}) that were used to produce a

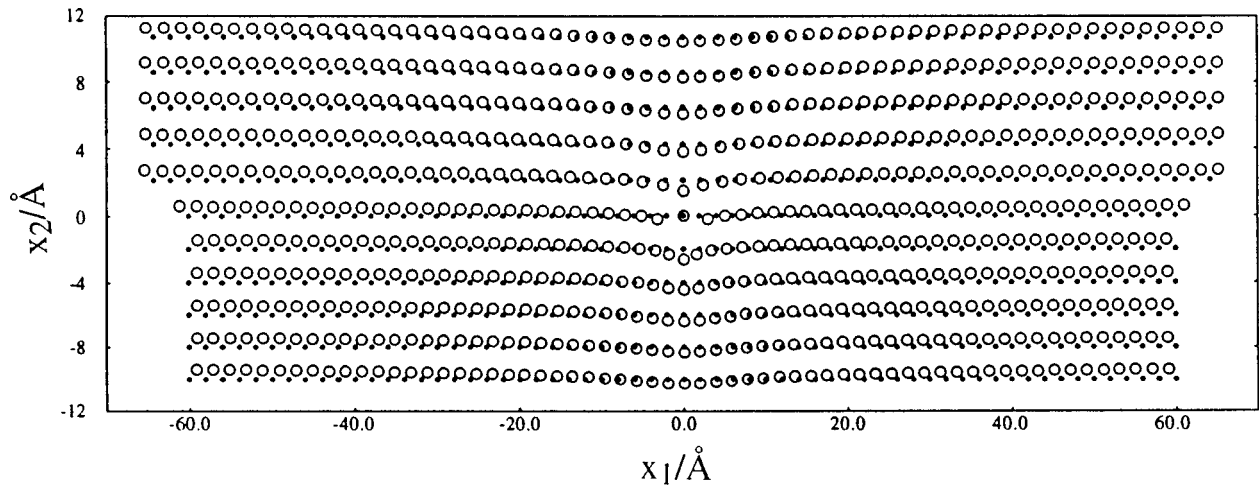


FIG. 5. The atomic displacement field obtained from classical elasticity theory, shown in [001] cross section (both atom species shown, In and As), and expanded by a factor of 2 in the x_2 direction for clarity. Small black dots: atom positions before displacement, open circles: atoms elastically displaced due to the dislocation strain field. The displacement for the epilayer atoms directly above the dislocation is negative.

TABLE I. Values of the epilayer Poisson ratio ν_{fit} used in the modified classical elasticity theory to fit the experimental values for the surface vertical displacement.

InAs film thickness/ML	ν_{fit}	$\nu_{\text{InAs}}/\nu_{\text{fit}}$
5	0.500	1.85
10	0.465	1.72
15	0.405	1.50
20	0.395	1.46
25	0.395	1.46
30	0.380	1.40

good fit to the experimental STM data for the surface vertical displacement. The value of ν_{fit} decreases with film thickness, becoming progressively more gradual at higher film thicknesses, i.e., the material becomes stiffer, but is always more deformable than would be experienced by using the bulk value, ν_{InAs} .

A second modification to classical elasticity theory has recently been reported by Springholz.¹³ The method of image dislocations was used to incorporate a relaxed, traction free surface into the theory. The expressions derived for the surface (nominally, $x_2=0$) displacement due to a single misfit dislocation at the interface ($x_2=-d$) are

$$u_1 = \frac{b}{\pi} \left[\frac{-dx_1}{x_1^2 + d^2} + \arctan\left(\frac{x_1}{d}\right) \right], \quad (3)$$

$$u_2 = \frac{b}{\pi} \left(\frac{d^2}{x_1^2 + d^2} \right). \quad (4)$$

These appear to be rather simple since no material specific elastic constants are featured and the vertical displacements depend only on the position with respect to the Burgers vector. Above the dislocation ($x_1=0$) on the surface, the expression for u_2 reduces to b/π and is therefore independent of film thickness. In the case of InAs/GaAs(110), $b/\pi = -1.36 \text{ \AA}$ and is clearly a large overestimate. This modified approach does, however, have an important advantage over the classical theory. In the classical elasticity theory approach, surface atoms some 5–6 lattice spacings along x_1 away from the dislocation (at $x_1=0$) are actually displaced *upwards* (Fig. 5), a phenomenon having no physical basis and a further indication that the theory is applicable only over very local distances. By contrast, the modified theory has surface atoms which are all displaced downwards, decreasing in magnitude to zero when significantly distant from the dislocation along x_1 .

This modified theory may be used to extract values for the lateral FWHM due to the vertical displacement. Although it still suffers from the fundamental limitation of containing only one dislocation, the more realistic behaviour just described can be used artificially to introduce extra dislocations adjacent to the core at the origin, to assess the contribution of the increasing FWHM to the decreasing vertical displacement in an array of dislocations. This is done simply by superimposing the displacements due to two theoretical adjacent dislocations at $x_1 = \pm \Lambda$, i.e., $u_2(x_1) = [u_2(x_1) + u_2(x_1 + \Lambda) + u_2(x_1 - \Lambda)]$ for $x_1 \geq 0$, or $u_2(x_1) = [u_2(x_1)$

$+ u_2(x_1 + \Lambda) + u_2(x_1 + \Lambda + 2|x_1|)]$ for $x_1 < 0$, respectively, based on the linear superposition principle of Saint-Venant.²⁷

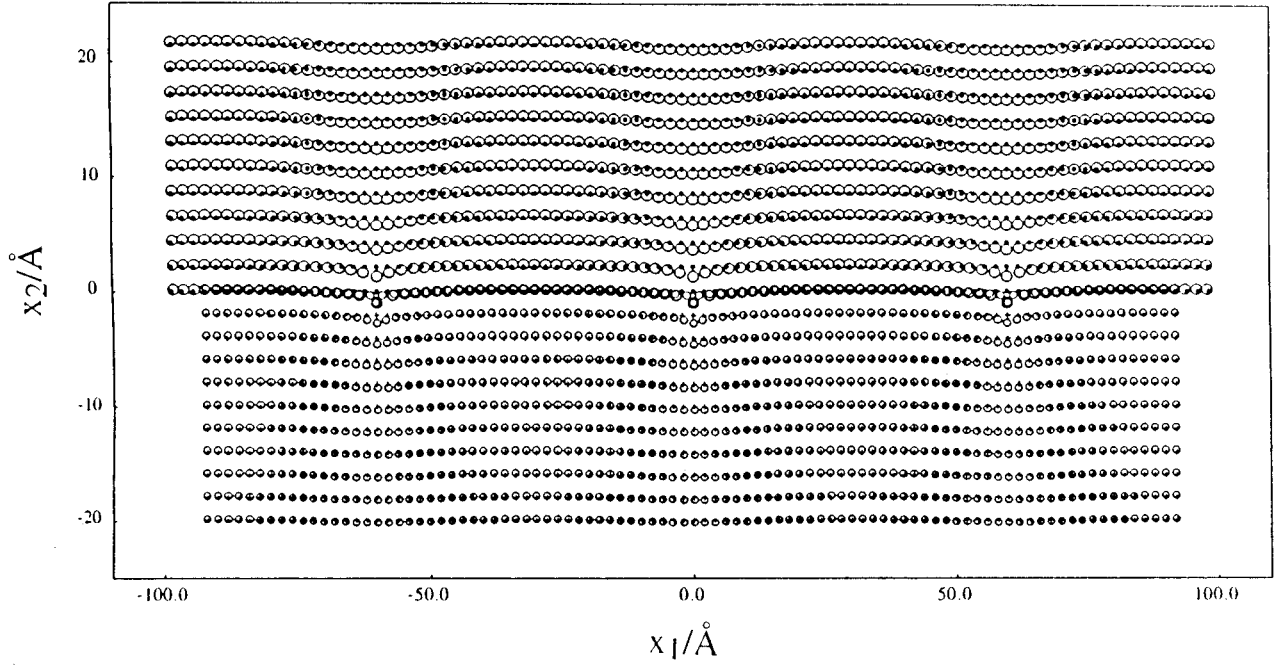
The corrugation and FWHM of the surface profiles obtained allow comparison with the experimental data, but they do not represent real surface displacements. For example, the vertical displacements range from -3.81 to -3.87 \AA for the surface of a 100-ML film, whereas for a real surface they should vary from 0.00 to -0.06 \AA . For the single dislocation, the vertical displacement is independent of film thickness [Fig. 2(a)] and equal to $b/\pi = -1.36 \text{ \AA}$; the FWHM [not shown in Fig. 2(b)] increases linearly, equal in magnitude to twice the film thickness (in ML). For the dislocation in between the two neighboring dislocations, the vertical displacement does indeed decrease in magnitude from -1.36 to -0.1 \AA by 30 ML. Simultaneously, the FWHM increases from 4 to 36 \AA at 30 ML (and 39 \AA at 100 ML; $\sim 40 \text{ \AA}$ appears to be a limiting figure). The plots for the triple dislocation array appear to be in reasonable agreement with the measured values and are also reproduced in Fig. 2. It is important to realize that in this case, the decreasing vertical displacement is due entirely to the increasing FWHM since it would remain constant for a single dislocation. The predicted vertical displacements exceed the experimental values for film thicknesses up to ~ 15 ML, while for greater film thicknesses the agreement is more reasonable (to within the STM resolution limit of $\sim 0.1 \text{ \AA}$). The deviation is most significant for film thicknesses less than 10 ML (0.2–0.6 \AA), an observation that is addressed later. The FWHM appears to have an upper limit of 35–40 \AA , in good agreement with the experimental behavior. This limiting value is only slightly in excess of half the dislocation separation, $\Lambda/2$, and the surface profile is best described as being *sinusoidal* in form.

C. Bonnet method

The final approach that has been made to define the surface atom displacement field is that set out by Bonnet.^{19,20} The theory uses a number of extra parameters compared to classical elasticity theory; (i) a free surface, where a parameter h represents the film thickness, and (ii) the option to have an array of dislocations with adjustable separation Λ [Fig. 4(b)]. The Burgers vector of the misfit dislocation can have any orientation with respect to the dislocation line \mathbf{u} , an edge component (b_1), a vertical component (b_2), and a screw component (b_3), although $b_2 = b_3 = 0$ in this case, since only b_1 is defined for an ideal edge dislocation. The elastic properties of the film and substrate are also better described and interdependent, with a Poisson ratio (ν) and shear modulus (μ) for each medium. These isotropic elastic quantities can be obtained from the tabulated anisotropic elastic constants (c_{11} , c_{12} , and c_{44} in a cubic crystal system) by a variety of averaging methods. The two simplest are the Voigt²⁸ and Reuss²⁹ methods, although more thorough treatments have also been proposed.³⁰ Of the two earlier methods, the Voigt averages are preferable for InAs/GaAs(110) since the values obtained are generally accepted as the most suitable for highly local dislocation strain properties. The elastic quantities employed here are $\nu = 0.25$, $\mu = 46.3 \text{ GPa}$ for GaAs and $\nu = 0.30$, $\mu = 29.2 \text{ GPa}$ for InAs.

The general expression for the displacement field u_k is defined as a complex Fourier series versus the coordinate x_1 , i.e.,

(a)



(b)

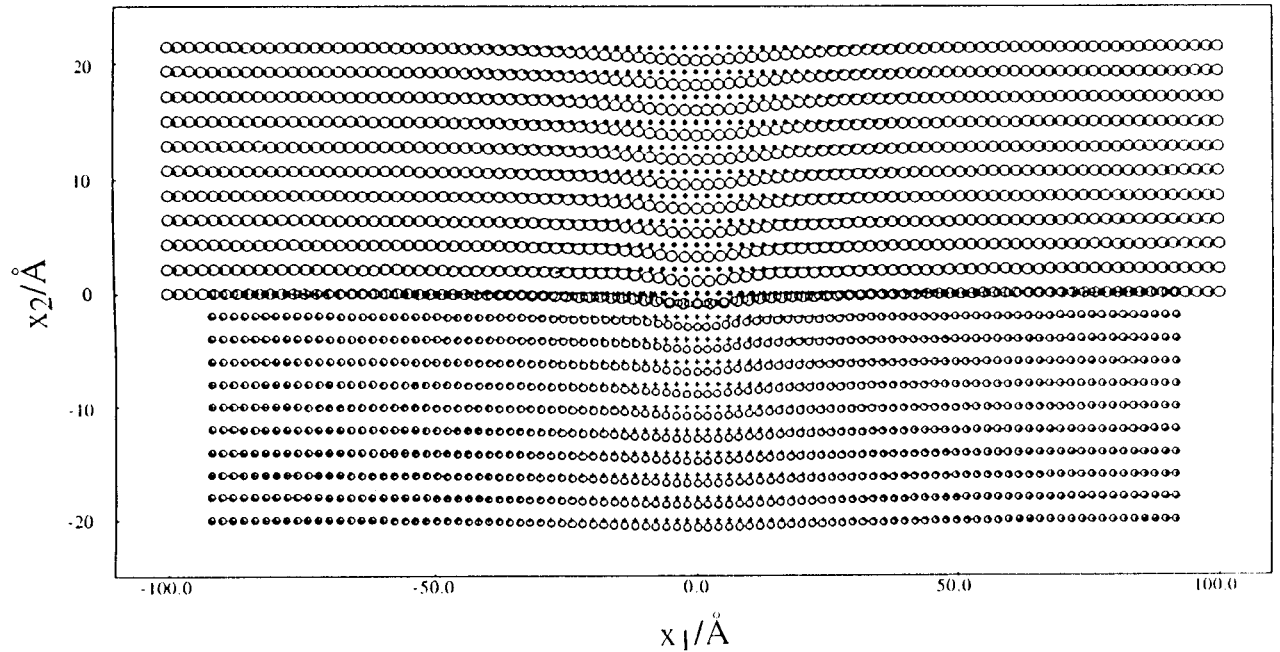


FIG. 6. The atomic displacement fields, in [001] cross section, obtained from the method of Bonnet (Sec. IV C): (a) close-packed dislocation array, $\Lambda = 60 \text{ \AA}$ and (b) a single dislocation, $\Lambda = 1000 \text{ \AA}$. The symbols illustrate the atomic positions before displacement in the GaAs substrate (crosses) and InAs film (black dots), and after elastic displacement due to the dislocation strain field (open circles).

$$u_k = \sum_{-\infty}^{\infty} U_k e^{im\omega x_1}, \quad (5)$$

where $\omega = 2\pi/\Lambda$ and U_k depends only on x_2 . Analytical solutions for u_1 and u_2 have been derived by Bonnet both for a multilayered structure with a number of heterointerfaces²⁰ and in the case of a thin film with a free surface.³¹ Some atomic displacement fields obtained from this method are

shown in Fig. 6, for (a) a section of a dislocation array and (b) an isolated dislocation. In each case, the displacements are largest close to the dislocation core and tend to zero at greater distances. As such, this is the first approach which predicts realistic atomic displacements throughout the entire crystal and is therefore more amenable to comparison with experiments. The values for the vertical displacement and FWHM obtained using a dislocation array, with $\Lambda = 60 \text{ \AA}$,

are very similar to the data obtained using the Springholz modification to classical elasticity theory.¹³ The vertical displacement is an overestimation of the experimental data below 10 ML, but is reasonable thereafter, while the FWHM is in good agreement and indicates a sinusoidal surface profile. The realistic surface displacements also show that the overall vertical displacement (i.e., that which should be compared with the STM data) is the *sum* of the *negative* displacement above the dislocation, $u_2(x_1=0, x_2=h)$ and a *positive* vertical displacement halfway in between the dislocations, $u_2(x_1=\Lambda/2, x_2=h)$ [Fig. 6(a)]. For thin layers (<10 ML), the negative displacement is the dominant contribution, while they become equal in magnitude for thicknesses >20 ML. The inclusion of a surface in the theory can also be tested and the vertical displacement in a given InAs layer is found to be greater when it is the surface layer than when it is somewhere inside the film. The similarity with the figures obtained from the Springholz method, which depends only on the Burgers vector, may be thought of as fortuitous, but decreasing the film elastic constants (ν, μ) in the Bonnet model by up to 50% yields relatively small (~10%) shifts in the magnitude of the vertical displacement.

The principle that large reductions (with the exception of the more simple classical elasticity theory, which requires an increase) in the elastic constants are required to bring the predicted vertical displacements towards the experimental data is very significant. A reduction in the Poisson ratio corresponds to making the epitaxial layer less deformable in the transverse (vertical) direction. It is important to remember that the average isotropic elastic parameters used in all three theories are based on the anisotropic elastic constants of the *bulk* material, but a thin, strained epitaxial layer will be much stiffer than the bulk if it contains misfit dislocations. For dislocations that compensate for compressive layer misfit strain, many interatomic bonds are stretched significantly beyond their ideal lengths in the lateral direction near the dislocation cores, an effect that would limit the capacity of these atoms to be displaced elastically in the vertical direction. Anomalous mechanical properties are well known in thin films and, in particular, the so-called *supermodulus effect*, or a hardening of the elastic properties by a factor of 100% or more in thin films, has been well documented,^{32,33} with the perturbation in atom positions due to interfacial stress invoked as the most likely cause for “very” thin (<50 Å) *incoherent* films.³⁴ The effect was predicted to disappear if the films were thin enough to be coherent, which implies that interfacial misfit dislocations are the cause of the disturbance in the atomic bond elastic properties.

The values obtained for the vertical displacement and FWHM, calculated by the Bonnet method for a *single* dislocation, are also rather intriguing [Figs. 2(a) and 2(b)]. A single dislocation is simulated by adopting a large dislocation spacing ($\Lambda=1000$ Å) so that each dislocation strain field is essentially independent [Fig. 6(b)]. In the classical theories, the vertical displacement for a single dislocation

either decays quickly ($\nu=\nu_{\text{InAs}}$), or remains constant at $u_2 = -0.68$ Å ($\nu=0.5$), or at $u_2=b/\pi=-1.36$ Å in the Springholz modification. In the Bonnet approach, the vertical displacement still decreases with film thickness, but much more slowly than for the dislocation array ($\Lambda=60$ Å). In the film thickness range up to 30 ML, the vertical displacement decreases by less than 1.2 to 1.0 Å, not actually reaching the STM resolution limit of 0.1 Å until some 300 ML thickness. It should be possible, therefore, to image isolated buried dislocations with an STM for more than 500 Å film thickness provided the large FWHM does not make them difficult to detect in the image. Such a long-range decay bears no resemblance to the rapid experimental decrease in vertical displacement, which must therefore be *predominantly a consequence of strain field superposition due to the increasing width of the strain fields originating from adjacent dislocations*. The FWHM for a single dislocation is also free to increase, whilst those for a $\Lambda=60$ Å array begin to saturate at 30–40 Å from ~15 ML.

V. CONCLUSIONS

The elastic displacement of atoms due to the edge dislocation strain field in InAs thin films grown on GaAs(110) have been assessed from STM measurements of the depth and lateral dimensions of the surface depressions formed as a consequence of the dislocations. The experimental data obtained for a wide range of film thicknesses (≤ 30 ML) has been modeled using a number of theoretical approaches based on classical theory and for satisfactory agreement, the theoretical models must contain a free epilayer surface. Although the Springholz modification to classical elasticity theory does provide reasonable agreement, the Bonnet model is the most powerful in terms of deriving realistic long range displacements. The decrease in surface vertical displacement is found largely to be a consequence of the increase in FWHM in a closely packed dislocation array. In a dislocation array, the FWHM soon attains a limiting magnitude that corresponds to about half the average dislocation spacing. The displacement profile is therefore best described as being sinusoidal in form. Significant deviations in the vertical displacement between the best theories and experiment were still observed for “ultrathin” films (<20 Å). This deviation reflects a greatly enhanced stiffness in the thin film, similar to the supermodulus effect identified in other materials systems. The stiffness can be explained by the high lateral atomic displacements near the misfit dislocation cores which limit the capacity of the film to further deformation.

ACKNOWLEDGMENTS

This work was supported by the EPSRC (UK) under Grant Nos. GR/J97540 and GR/K23775. EPSRC is also thanked for support to J.G.B. We are very grateful to Roland Bonnet for discussions regarding his model.

*FAX: ++44(0)171 594 5801. Electronic address: t.jones@ic.ac.uk

¹A. Vilà, A. Coronet, J. R. Morante, P. Ruterana, R. Bonnet, and M. Loubradou, *Inst. Phys. Conf. Ser.* **146**, 83 (1995).

²G. Meyer, B. Voigtländer, and N. M. Amer, *Surf. Sci.* **274**, L541 (1992).

³R. Stalder, H. Siringhaus, N. Onda, and H. van Känel, *Ultramicroscopy* **42-44**, 781 (1992).

- ⁴N. Frank, G. Springholz, and G. Bauer, Phys. Rev. Lett. **73**, 2236 (1994).
- ⁵H. Yamaguchi, J. G. Belk, X. M. Zhang, J. L. Sudijono, M. R. Fahy, T. S. Jones, D. W. Pashley, and B. A. Joyce, Phys. Rev. B **55**, 1337 (1997).
- ⁶J. G. Belk, J. L. Sudijono, H. Yamaguchi, X. M. Zhang, D. W. Pashley, C. F. McConville, T. S. Jones, and B. A. Joyce, J. Vac. Sci. Technol. A **15**, 915 (1997).
- ⁷R. Stalder, H. Sirringhaus, N. Onda, and H. van Känel, Appl. Phys. Lett. **59**, 1960 (1991).
- ⁸M. Schmid, A. Biedermann, H. Stalder, and P. Varga, Phys. Rev. Lett. **69**, 925 (1992).
- ⁹G. Ritz, M. Schmid, A. Biedermann, and P. Varga, Phys. Rev. B **53**, 16 019 (1996).
- ¹⁰B. Voigtländer and A. Zinner, J. Vac. Sci. Technol. A **12**, 1932 (1994).
- ¹¹G. Springholz, G. Bauer, and V. Holy, Phys. Rev. B **54**, 4500 (1996).
- ¹²G. Springholz, G. Bauer, and V. Holy, Surf. Sci. **365**, 453 (1996).
- ¹³G. Springholz, Appl. Surf. Sci. **112**, 12 (1997).
- ¹⁴H. Bethge, D. Heuer, Ch. Jensen, K. Reshöft, and U. Köhler, Surf. Sci. **331-333**, 878 (1995).
- ¹⁵X. Zhang, D. W. Pashley, L. Hart, J. H. Neave, P. N. Fawcett, and B. A. Joyce, J. Cryst. Growth **131**, 300 (1993).
- ¹⁶J. G. Belk, D. W. Pashley, C. F. McConville, B. A. Joyce, and T. S. Jones, Surf. Sci. **410**, 82 (1998).
- ¹⁷B. A. Joyce, J. L. Sudijono, J. G. Belk, H. Yamaguchi, X. M. Zhang, H. T. Dobbs, A. Zangwill, D. D. Vvedensky, and T. S. Jones, Jpn. J. Appl. Phys., Part 1 **36**, 4111 (1997).
- ¹⁸J. G. Belk, J. L. Sudijono, X. M. Zhang, J. H. Neave, T. S. Jones, and B. A. Joyce, Phys. Rev. Lett. **78**, 475 (1997).
- ¹⁹R. Bonnet, Philos. Mag. A **43**, 1165 (1981).
- ²⁰R. Bonnet, Phys. Rev. B **53**, 10 978 (1996).
- ²¹D. M. Holmes, J. G. Belk, J. L. Sudijono, J. H. Neave, T. S. Jones, and B. A. Joyce, J. Vac. Sci. Technol. A **14**, 849 (1996).
- ²²D. M. Holmes, J. G. Belk, J. L. Sudijono, J. H. Neave, T. S. Jones, and B. A. Joyce, Surf. Sci. **341**, 133 (1995).
- ²³F. R. N. Nabarro, *Theory of Crystal Dislocations* (Oxford University Press, New York, 1967), p. 641.
- ²⁴J. P. Hirthe and J. Lothe, *Theory of Dislocations* (Krieger, Malabar, 1992), p. 68.
- ²⁵W. Spirkl, B. K. Tanner, C. Whitehouse, S. J. Barnett, A. G. Cullis, A. D. Johnson, A. Keir, B. Usher, G. F. Clark, W. Hagston, C. R. Hogg, and B. Lunn, Philos. Mag. A **70**, 531 (1994).
- ²⁶B. Devincre, Solid State Commun. **93**, 875 (1995).
- ²⁷S. Timoshenko and J. N. Goodier, *Theory of Elasticity* (McGraw-Hill, New York, 1951), p. 33.
- ²⁸W. Voigt, *Lehrbuch der Kristalphysik* (Teubner, Leipzig, 1928), p. 716.
- ²⁹A. Reuss, Z. Angew. Math. Mech. **9**, 55 (1929).
- ³⁰N. Fribourg-Blanc, M. Dupeux, G. Guenin, and R. Bonnet, J. Appl. Crystallogr. **12**, 151 (1979).
- ³¹R. Bonnet and J. L. Verger-Gaugry, Philos. Mag. A **66**, 849 (1992).
- ³²W. M. C. Yang, T. Tsakalakos, and J. E. Hilliard, J. Appl. Phys. **48**, 876 (1977).
- ³³U. Helmersson, S. Todorova, S. A. Barnett, and J.-E. Sundgren, J. Appl. Phys. **62**, 481 (1987).
- ³⁴R. C. Cammarata and K. Sieradzki, Phys. Rev. Lett. **62**, 2005 (1989).